Thin Solid Films 577 (2015) 143–148

Contents lists available at ScienceDirect

Thin Solid Films

journal homepage: www.elsevier.com/locate/tsf

Defect-sealing of Al_2O_3/ZrO_2 multilayer for barrier coating by plasma-enhanced atomic layer deposition process

Jong Geol Lee [a], Hyun Gi Kim [b], Sung Soo Kim [a,b,*]

[a] Department of Chemical Engineering, Kyung Hee University, Yongin-si, Gyeonggi-do 446-701, Republic of Korea
[b] Regional Innovation Center-Components and Materials for Information Display, Kyung Hee University, Yongin-si, Gyeonggi-do 446-701, Republic of Korea

ARTICLE INFO

Article history:
Received 16 May 2014
Received in revised form 21 January 2015
Accepted 21 January 2015
Available online 28 January 2015

Keywords:
Diffusion barrier
Plasma-enhanced atomic layer deposition
Defect-sealing
Aluminum oxide
Zirconium oxide
Multilayer

ABSTRACT

Barrier layers were coated by plasma enhanced atomic layer deposition. They had inevitable defects for several reasons and these defects deteriorated the diffusion barrier properties. The size of the pinhole defect decreased with the increase of the layer thickness resulting in enhanced barrier properties, until the thickness reached 20 nm for a single-component aluminum oxide (Al_2O_3) or zirconium oxide (ZrO_2) layer. No more enhancement of barrier properties was observed with a further increase of layer thickness, since the defects tended to grow in single-component layers. Alternation of Al_2O_3 and ZrO_2 layers prevented defect growth by covering the defects with another component, and enhanced the barrier properties when compared with single-component layers. Increase of the number of Al_2O_3/ZrO_2 stacks with the same total layer thickness remarkably reduced the water vapor transmission rates value to below 5×10^{-5} g/m^2 day at 38 °C and 100% relative humidity. The Al_2O_3/ZrO_2 multilayer formed on a polyethylene naphthalate substrate at optimized conditions showed light transmittance greater than 86% at a wavelength of 550 nm, for application as flexible display substrate.

1. Introduction

For the substitution of a conventional glass substrate with plastic substrate in flexible organic light emitting diodes (FOLED), it is essential to acquire high performance passivation such as encapsulation and a gas barrier [1]. Permeation of atmospheric gases such as water vapor and oxygen through a plastic substrate can corrode the organic materials and the metallic cathode, which results in the reduction of the electron injection in FOLED devices and deteriorates their performance and lifetime [2]. Therefore, a gas barrier layer is required for plastic substrates, to prevent the diffusion of both water vapor and oxygen, and the water vapor transmission rates (WVTR) must be less than 10^{-5} g/m^2 day. For these reasons, barrier layers such as vacuum-deposited inorganic thin films have been extensively explored for improvement of the long-term stability of FOLED devices [3].

However, thin films formed by a vacuum deposition process can have defects that provide a pathway for water vapor and oxygen through the substrate, because deposition techniques and defect-free coating are not perfect [4]. Even though sample handling is performed in a clean room atmosphere, defects such as pinholes and voids are generated from the imperfect structure of the inorganic thin film during the deposition process. For sealing defects and suppressing the diffusion rate, multilayer structures of inorganic/inorganic layers have been proposed [5]. Defects of an inorganic layer are closed by another inorganic layer, which avoids the propagation of pinholes from one layer to another and results in the increase of the time needed for permeation of vapor through the barrier layer. Vapor molecules need to laterally diffuse through the interface of the layers from a defect of an inorganic layer to another defect of the next layer [6]. Research reports indicate that a multilayer structure with inorganic/inorganic stacks shows a better barrier performance than that of a single-component layer structure [7].

Recently, several research works focused on improving barrier performance using a multilayer structure of alternating inorganic materials such as aluminum oxide (Al_2O_3), silicon oxide, titanium oxide, zinc oxide and zirconium oxide (ZrO_2) [7–9]. Among these inorganic materials, multilayers consisting of Al_2O_3 and ZrO_2 showed better barrier properties than the others [10,11]. Although there have been extensive studies of gas barrier layers with an inorganic/inorganic multilayer structure, most of them focused on the mechanism of barrier properties using a Ca-test method [12]. There is little research that has studied direct observations of how a defect of an inorganic layer would be affected by another inorganic layer.

In this study, single-component layer of Al_2O_3 or ZrO_2 was formed on polyethylene naphthalate (PEN) substrates by low-frequency plasma-enhanced atomic layer deposition (PEALD) process, and characteristics of each layer were examined. Defect growth in a single-component layer was examined, and the defect filling mechanism of layer deposition of another component was traced by using field

* Corresponding author at: Department of Chemical Engineering, Kyung Hee University, Yongin-si, Gyeonggi-do 446-701, Republic of Korea. Tel.: +82 31 201 3257; fax: +82 31 204 3294.
E-mail address: sungkim@khu.ac.kr (S.S. Kim).

http://dx.doi.org/10.1016/j.tsf.2015.01.040
0040-6090/

emission transmission electron microscope (FE-TEM) techniques. The WVTR value of the Al_2O_3/ZrO_2 multilayer was compared with those of single-component layers. Effects of the number of Al_2O_3/ZrO_2 stacks were also examined.

2. Experimental details

Al_2O_3 and ZrO_2 layers were deposited on PEN substrates by using low frequency PEALD located in a class 10,000 clean room. The PEALD equipment used in this work has been described in our previous work [13]. Argon gas of 99.999% purity was continuously introduced into the deposition chamber at a flow rate of 500 sccm, while it built up the background pressure at 53.3 Pa. Argon gas was also used as the carrier gas for the precursor and reactant vapor as well as for the purge gas after each cycle. The PEN substrate was type Q65 from DuPont-Teijin Films, and its thickness was 125 μm.

Trimethylaluminum (TMA) was used as a precursor for Al_2O_3 layer formation and tetrakis(ethylmethylamino)zirconium (TEMAZ) was used for ZrO_2 layer formation; oxygen was used as a reactant material. Since TEMAZ has a high boiling temperature, it was maintained at 80 °C during the deposition process, while TMA was at 20 °C. The substrate was maintained at 120 °C in the chamber during the deposition process for all the samples. Prior to deposition of the barrier layer, the PEN substrates were cleaned in a sonicated isopropyl alcohol bath for 20 min and were dried at 80 °C for 120 min in the convection oven to remove residual water. For the Al_2O_3 deposition, the one cycle consisted of the sequential injection of a TMA pulse (1.0 s), Ar purge (5.0 s), oxygen pulse (4.0 s) and Ar purge (5.0 s). One cycle of ZrO_2 deposition consisted of the sequential injection of a TEMAZ pulse (1.5 s), Ar purge (6.0 s), oxygen pulse (5.0 s) and Ar purge (6.0 s). A radio frequency (RF) plasma pulse which was capacitively coupled with a low frequency (500 kHz) plasma source was applied for 3.0 s only during the oxygen pulse, to produce oxygen radicals. The RF plasma power was 300 W, and the electrode-substrate distance was 50 mm, as optimized in previous work [13].

The Al_2O_3/ZrO_2 multilayers were fabricated by alternating the deposition of Al_2O_3 and ZrO_2 layers. The Al_2O_3 layer was first deposited on the cleaned PEN substrate at a certain thickness, which was determined by the number of process cycles. Then the ZrO_2 layer was deposited onto the Al_2O_3 layer with the same number of process cycles. While the total thickness was fixed, the multilayer was prepared with various numbers of Al_2O_3/ZrO_2 stacks of different stack thicknesses. Various numbers of stacks were tested, from one to five stacks.

The WVTR values for the barrier layer fabricated on the PEN substrate were determined at 38 ± 1 °C and 100% relative humidity (RH) using the AQUATRAN Model 2 (MOCON Inc.) for 72 to 720 h, depending on the barrier's properties. After each sample was loaded, we traced the WVTR value until it reached the steady state. More time for stabilization was needed for a high barrier property sample. We double-checked the barrier properties of the sample by a Calcium cell test, and based on the results of the test, we could confirm the validity of the measurement time in the MOCON apparatus. The detection limit of the AQUATRAN Model 2 instrument was 5×10^{-5} g/m^2 day.

The thickness and refractive index of the Al_2O_3 and ZrO_2 single layers were measured by spectroscopic ellipsometry (V-VASE, J. A. Woollam. Co.). The optical transmittance of each sample was measured in the wavelength range from 350 to 800 nm by a UV/visible spectrometer (MCPD-3000, Otsuka Co.). The surface and cross-section morphology of the Al_2O_3/ZrO_2 multilayer were obtained by FE-TEM (JEM-2100F, JEOL Ltd.) working at an accelerating voltage of 200 kV. For the measurement of surface morphology, the layers were directly deposited on 300 mesh Cu-grids (3 mm diameter grid coated with carbon supported film, Ted Pella, Inc.). For the measurement of cross-sectional morphology, the samples were fabricated by using a focused ion beam (FIB) system (NOVA 200, FEI Co.).

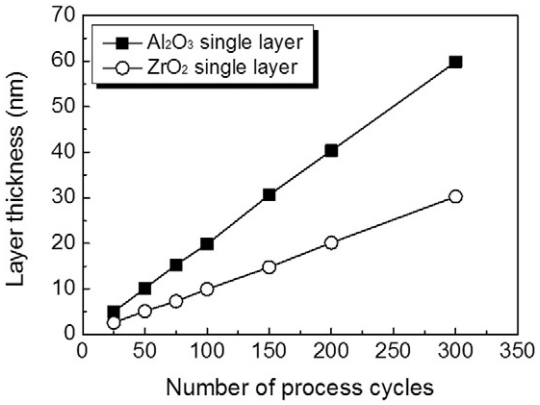

Fig. 1. Layer thickness variations of Al_2O_3 and ZrO_2 single component layer with the number of process cycle.

3. Results and discussion

Fig. 1 shows that the layer thickness linearly increased with the number of process cycles for both the Al_2O_3 and ZrO_2 single layers deposited on the PEN substrate. In the atomic layer deposition (ALD) process, the growth rate of a layer depended more on the number of process cycles than on the cycle time or the intensity of the material pulse. This result was only obtained at the process condition that dominated the growth mechanism of the ALD processes by a self-limiting reaction of surface adsorption [14]. The growth rates for the Al_2O_3 and ZrO_2 layers were obtained from the total layer thickness divided by the number of process cycles, the rates were found to be 0.21 nm/cycle for the Al_2O_3 layer and 0.11 nm/cycle for the ZrO_2 layer. The value for Al_2O_3 layer is greater than that of the typical ALD process using H_2O as a reactant material, due to a more efficient surface oxidation by plasma-generated oxygen radicals compared to thermally activated oxidation by H_2O [15]. Having a lower growth rate for the ZrO_2 layer than for the Al_2O_3 layer could be attributed to steric hindrance caused by the large TEMAZ [$Zr(NCH_3C_2H_5)_4$] admolecule on the surface of the substrate [16].

We had a purging step with argon for 5 s after $Al(CH_3)_3$ feeding to discharge the unadsorbed $Al(CH_3)_3$ from the reactor. Oxygen radicals remaining after the reaction and the reaction product such as CH_3, CH_4 and H_2O were discharged from the reactor by another purging step with argon for 5 s as a final step of the cycle to prevent the defect formation by geometric shadowing effects. Therefore, we could avoid the parasitic chemical vapor deposition and non line-of-sight and geometric shadowing.

The barrier properties of the Al_2O_3 and ZrO_2 single layers were measured at various layer thicknesses, as shown in Fig. 2. WVTR values

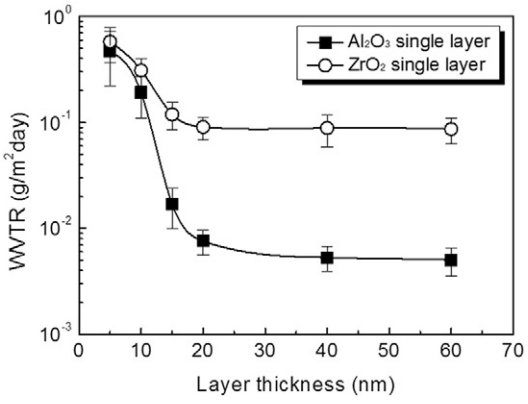

Fig. 2. WVTR variations of Al_2O_3 and ZrO_2 single component layers with the number of process cycle.

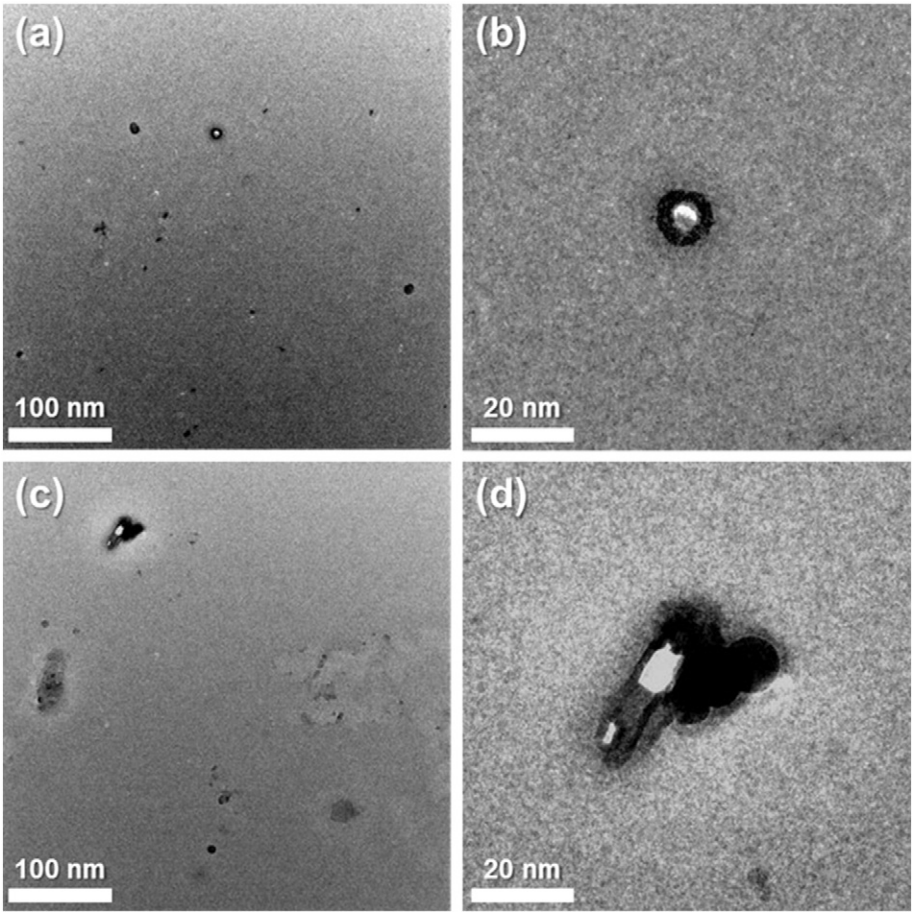

Fig. 3. FE-TEM image of Al_2O_3 and ZrO_2 single component layers with thickness of 50 nm deposited on Cu-grids; (a) low magnification of Al_2O_3 layer, (b) high magnification of Al_2O_3 layer, (c) low magnification of ZrO_2 layer, (d) high magnification of ZrO_2 layer.

of both single layers were not satisfactory for application to a flexible display, and they should be further improved. WVTR values decreased with increasing layer thickness in both cases until they reached a thickness around 20 nm. No more decreases of WVTR values were observed beyond 20 nm of thickness. There are several reasons for a limitation of WVTR decrease, such as layer density and defect formation in the layer. A saturation of barrier properties with increasing layer thickness can be attributed to a defect-dominated gas diffusion caused by pinholes [17]. Many defects exist in most deposited thin films due to the intrinsic properties of vacuum deposition, and these defects allow the permeation of water vapor and oxygen, resulting in the deterioration of barrier performance [18].

WVTR values of the Al_2O_3 single layer were lower than those of the ZrO_2 single layer, and they depended on the layer density as well as on the defects of each layer. For a morphological characterization of defects, the Al_2O_3 and ZrO_2 layers were directly deposited on

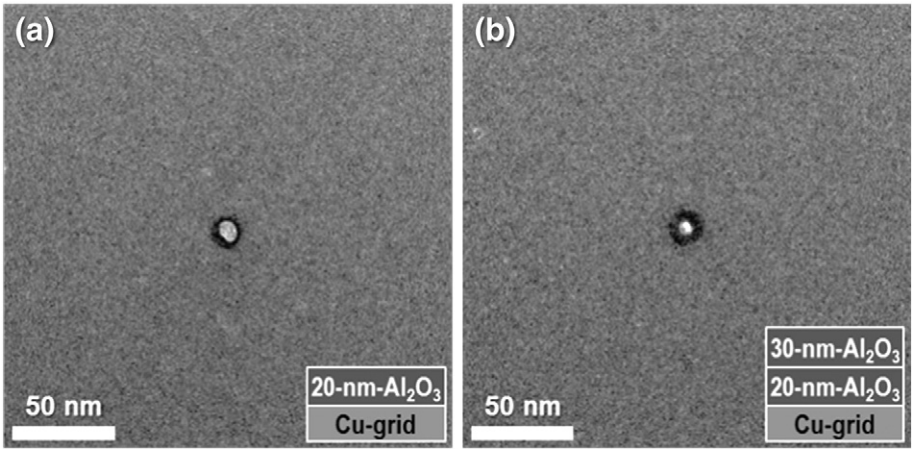

Fig. 4. FE-TEM images of Al_2O_3 single component layer; (a) initial 20 nm deposition of Al_2O_3, (b) additional 30 nm deposition of Al_2O_3 onto the 20-nm-Al_2O_3. (Same defect spot was traced after the FE-TEM analysis.).

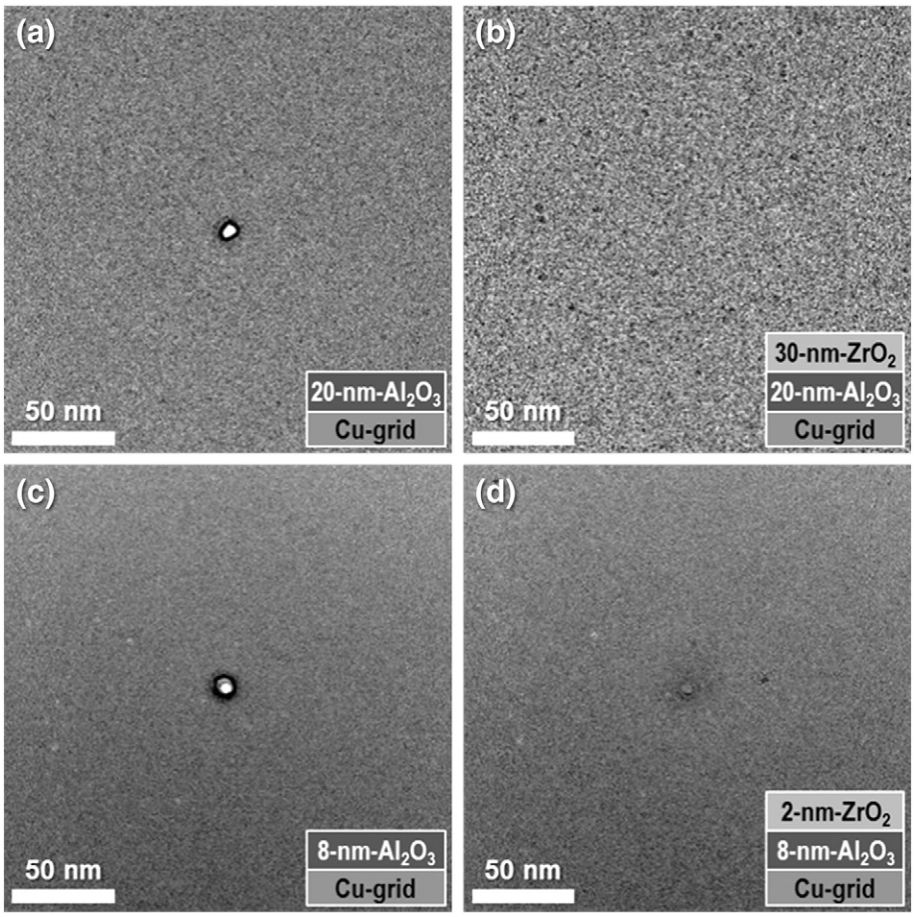

Fig. 5. FE-TEM images of Al_2O_3/ZrO_2 multilayer; (a) initial 20 nm deposition of Al_2O_3, (b) additional 30 nm deposition of ZrO_2 onto the 20-nm-Al_2O_3, (c) initial 8 nm deposition of Al_2O_3, (d) additional 2 nm deposition of ZrO_2 onto the 8-nm-Al_2O_3. (Same defect spot was traced after the FE-TEM analysis.).

300 mesh Cu-grids. In Fig. 3, FE-TEM images of Al_2O_3 and ZrO_2 layers with a thickness of 50 nm reveal that both layers have defects such as voids and pinholes. In principle, a perfect layer only a few nanometers thick should reduce the diffusion of water vapor and oxygen to acceptable levels. However, in practice, thin film coatings tend to have defects that provide easy paths for the permeation of water vapor and oxygen [19]. Although the ALD method was known as a defect-free process, defects were inevitably generated from the imperfect structure of the inorganic thin film during the deposition process [20]. These defects were known to be caused by particles on the substrate surface or by geometric shadowing and stress during film growth at sites of high surface roughness [17]. For permeation of water vapor and oxygen through defects, we focused on permeation through pinhole defects, which is more dominant than other defects such as void and grain boundary [21].

The effect of layer thickness in covering the defect was examined. An Al_2O_3 layer of 20 nm was deposited on a Cu-grid, and its defect was observed by using FE-TEM, as shown in Fig. 4(a). After FE-TEM analysis, a further Al_2O_3 layer of 30 nm thickness was deposited on the same sample shown in Fig. 4(a), at the identical deposition conditions. The same defect spot was traced, as shown in Fig. 4(b), and it was confirmed that the defect still remained after the additional deposition, even though the size of the defect was slightly decreased.

Many efforts were made to minimize the exposure effects of air and humidity while switching the sample between PEALD and FE-TEM. After the PEALD process, we stabilized the samples in a load-lock

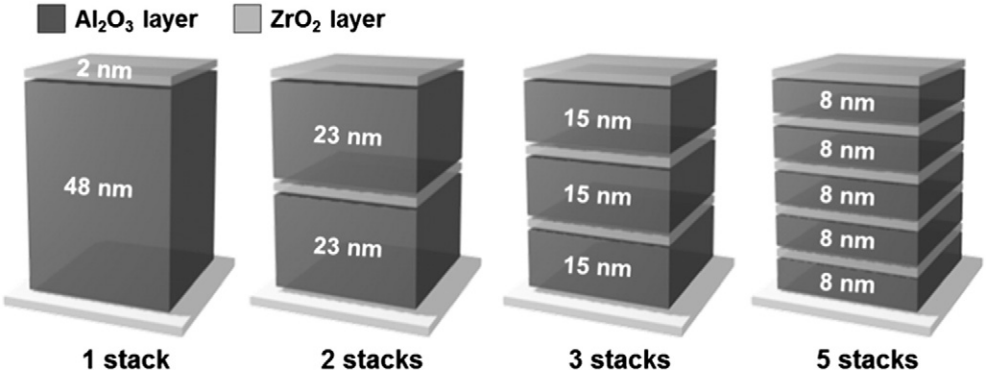

Fig. 6. Schematic diagrams various Al_2O_3/ZrO_2 multilayer stacks fabricated on PEN substrates. (Total thickness was fixed at 50 nm for every sample.).

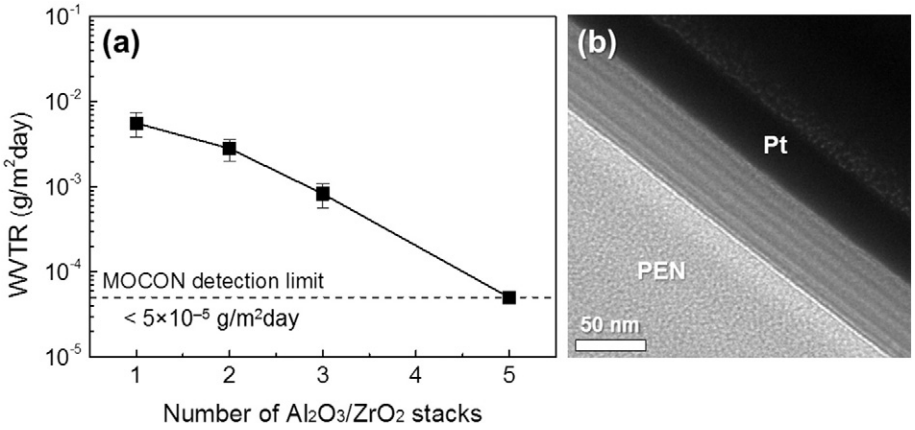

Fig. 7. (a) WVTR value variation of Al_2O_3/ZrO_2 multilayer with the number of Al_2O_3/ZrO_2 stacks and (b) Cross-sectional FE-TEM image of Al_2O_3(8 nm)/ZrO_2(2 nm)-5-stack multilayer on PEN substrate prepared by FIB technique.

chamber filled with Ar until they returned to ambient temperature, to avoid a sudden temperature change when saving the sample from the PEALD apparatus. The samples were stored in an Ar-filled container before loading in the FE-TEM. The interval between PEALD and FE-TEM was minimized to less than 10 min. The same procedure was applied when switching the sample from FE-TEM to PEALD. We tried to determine whether extra defects were formed after exposure to air and humidity. No extra defects were detected after the second PEALD process, and we confirmed that the surfaces were not seriously damaged during the exposure.

The presence of a defect allowed the permeation of water vapor to result in the saturation of the WVTR value beyond the thickness of 20 nm, as shown in Fig. 2. According to the reported studies, as the thickness of the layer increases, the size and density of defects decrease, and consequently, the WVTR value decreases as well [22]. However, when the thickness reached a critical value, the density of the defect could not decrease further, and the WVTR would become saturated. Thus, an organic–inorganic composite layer was proposed to overcome the defect problems by covering the organic material layer and supplementing with an inorganic single-barrier layer [6]. However, the density of the organic layer is much less than that of the inorganic layer, and filling the defect with organic material may not be as efficient as doing so with inorganic materials.

Similar defect covering work was performed by the deposition of a ZrO_2 layer of 30 nm on the Al_2O_3 layer of 20 nm on the Cu-grid. A defect image from the Al_2O_3 layer of 20 nm on the Cu-grid was obtained, as shown in Fig. 5(a); it was quite similar to that in Fig. 4(a), because both samples were prepared under the same conditions. The same defect spot was traced after the deposition of the ZrO_2 layer, as shown in Fig. 5(b), and it was confirmed that the defect was covered by the ZrO_2 layer. Therefore, it could be concluded that once defects are formed, for whatever reason, those defects tend to grow if the same material is deposited, regardless of the amount deposited. But a defect's growth can be suspended by the deposition of another material, and alternating deposition may form defect-free layers. It was also expected that barrier properties could be enhanced by making an Al_2O_3/ZrO_2 multilayer when compared with only a single Al_2O_3 layer, even though both samples had the same layer thickness of 50 nm. The thickness of each layer was reduced to 8 nm for the Al_2O_3 layer and to 2 nm for the ZrO_2 layer, and the FE-TEM images revealed that the defect was covered, as shown in Fig. 5(c) and (d). It was confirmed that the defect covering effect of the ZrO_2 layer on the Al_2O_3 layer was valid at reduced thickness.

Therefore, we fabricated an Al_2O_3/ZrO_2 multilayer with various numbers of stacks, while the total layer thickness was fixed at 50 nm by reducing the thickness of the Al_2O_3 layer, as shown in Fig. 6. The thickness of the ZrO_2 layer, to be used as an interlayer, was fixed at 2 nm. The ZrO_2 layer tended to form a polycrystalline structure when its thickness exceeded 4 nm [11], and the polycrystalline structure reduced the flexibility of the barrier layer. Therefore, 2 nm was optimum in terms of the uniformity of the layer throughout the sample surface and of the flexibility for the plastic substrate.

The WVTR values of the Al_2O_3/ZrO_2 multilayer as a function of the number of stacks is shown in Fig. 7(a). The WVTR value decreased significantly with the increased number of stacks, and the 5-stack sample showed the lowest WVTR value of less than 5×10^{-5} g/m^2 day, which is the measurement limitation of the MOCON device. Increasing the number of stacks should enhance the probability of the defect filling effect, even though the thickness of each Al_2O_3 layer is reduced. A bending test was performed according to ASTM D522-93a, in order to examine the flexibility of the sample [23]. The 5-stack Al_2O_3/ZrO_2 multilayer sample underwent 5000-time cyclic bending around the radius of 2 cm. The sample retained its barrier properties after the bending test. Both the original sample and the sample after the bending test showed WVTR values less than the detection limit of the MOCON system (5×10^{-5} g/m^2 day) to confirm the flexibility of the sample.

Fig. 7(b) is a cross-sectional FE-TEM image of a 5-stack sample of an Al_2O_3(8 nm)/ZrO_2(2 nm) multilayer deposited on the PEN substrate. For cross-sectional measurement of the multilayers, the sample was fabricated by using FIB. A cross-sectional image of a 5-stack sample revealed that each layer was uniformly deposited on the PEN substrate.

The transmittance of the Al_2O_3/ZrO_2 multilayer as a function of the number of Al_2O_3/ZrO_2 stacks is shown in Fig. 8, and the transmittance

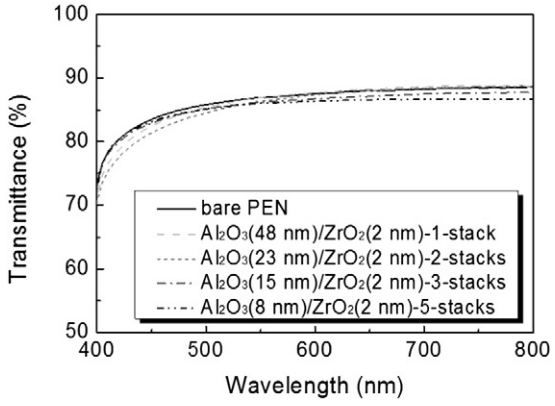

Fig. 8. Light transmittance variation of Al_2O_3/ZrO_2 multilayer deposited on PEN substrate with the number of Al_2O_3/ZrO_2 stacks.

through the air was used as a reference. It was generally expected that an increased number of layers would tend to reduce the transmittance due to the difference in the refractive index. However, an Al_2O_3/ZrO_2 multilayer fabricated for this study had a transmittance of 86% or above at the wavelength of 550 nm.

4. Conclusion

Barrier properties of Al_2O_3 and ZrO_2 single layers decreased with the increase of layer thickness, due to the defect size reduction, until the barrier reached the critical thickness. However, no more reduction of the WVTR value was observed beyond the critical thickness due to the presence of pinhole defects for a single-component layer. Defect trace work using FE-TEM revealed that the defect was growing when the single-component layer was deposited, no matter how much the layer thickness increased beyond its critical thickness. However, defect growth was suspended when ZrO_2 was deposited on an Al_2O_3 layer. Even a very thin ZrO_2 layer of 2 nm thickness could fill the defect of an Al_2O_3 layer of 8 nm. The WVTR value decreased continuously with the increased number of Al_2O_3/ZrO_2 stacks, when the total thickness of each sample was fixed at 50 nm. An Al_2O_3/ZrO_2 multilayer with 5-stacks attained a WVTR value below 5×10^{-5} g/m^2 day at 38 °C and 100% RH and the sample retained the original WVTR value after bending test, which ensured its application to a plastic substrate for flexible display. The sample showed a light transmittance greater than 86% at 550 nm wavelength after alternating depositions of Al_2O_3 and ZrO_2 layers.

Acknowledgment

This research was supported by a grant from the Fundamental R&D Program for Technology of World Premier Materials and the RIC-CAMID of Kyung Hee University.

References

[1] J.A. Jeong, H.K. Kim, M.S. Yi, Effect of Ag interlayer on the optical and passivation properties of flexible and transparent $Al_2O_3/Ag/Al_2O_3$ multilayer, Appl. Phys. Lett. 93 (2008) 033301.
[2] P.F. Carcia, R.S. McLean, M.D. Groner, A.A. Dameron, S.M. George, Gas diffusion ultrabarriers on polymer substrates using Al_2O_3 atomic layer deposition and SiN plasma-enhanced chemical vapor deposition, J. Appl. Phys. 106 (2009) 023533.
[3] S.-W. Seo, E. Jung, C. Lim, H. Chae, S.M. Cho, Moisture permeation through ultrathin TiO_2 films grown by atomic layer deposition, Appl. Phys. Express 5 (2012) 035701.
[4] Y. Zhang, Y.-Z. Zhang, D.C. Miller, J.A. Bertrand, S.H. Jen, R. Yang, M.L. Dunn, S.M. George, Y.C. Lee, Fluorescent tags to visualize defects in Al_2O_3 thin films grown using atomic layer deposition, Thin Solid Films 517 (2009) 6794.
[5] J. Meyer, P. Görrn, F. Bertram, S. Hamwi, T. Winkler, H. Johannes, T. Weimann, P. Hinze, T. Riedl, W. Kowalsky, Al_2O_3/ZrO_2 nanolaminates as ultrahigh gas-diffusion barriers — a strategy for reliable encapsulation of organic electronics, Adv. Mater. 21 (2009) 1845.
[6] A. Morlier, S. Cros, J.P. Garandet, N. Alberola, Gas barrier properties of solution processed composite multilayer structures for organic solar cells encapsulation, Sol. Energy Mater. Sol. Cells 115 (2013) 93.
[7] D.-W. Choi, S.-J. Kim, J.H. Lee, K.-B. Chung, J.-S. Park, A study of thin film encapsulation on polymer substrate using low temperature hybrid ZnO/Al_2O_3 layers atomic layer deposition, Curr. Appl. Phys. 12 (2012) S19.
[8] J.-H. Choi, Y.-M. Kim, Y.-W. Park, T.-H. Park, J.-W. Jeong, H.-J. Choi, E.-H. Song, J.-W. Lee, C.-H. Kim, B.-K. Ju, Highly conformal SiO_2/Al_2O_3 nanolaminate gas-diffusion barriers for large-area flexible electronics applications, Nanotechnology 21 (2010) 475203.
[9] T.-S. Kwon, D.-Y. Moon, Y.-K. Moon, W.-S. Kim, J.-W. Park, Al_2O_3/TiO_2 multilayer passivation layers grown at low temperature for flexible organic devices, J. Nanosci. Nanotechnol. 12 (2012) 3696.
[10] J. Meyer, H. Schmidt, W. Kowalsky, T. Riedl, A. Kahn, The origin of low water vapor transmission rates through Al_2O_3/ZrO_2 nanolaminate gas-diffusion barriers grown by atomic layer deposition, Appl. Phys. Lett. 96 (2010) 243308.
[11] S.-W. Seo, E. Jung, H. Chae, S.M. Cho, Optimization of Al_2O_3/ZrO_2 nanolaminate structure for thin-film encapsulation of OLEDs, Org. Electron. 13 (2012) 2436.
[12] R. Paetzold, A. Winnacker, D. Henseler, V. Cesari, K. Heuser, Permeation rate measurements by electrical analysis of calcium corrosion, Rev. Sci. Instrum. 74 (2003) 5147.
[13] J.G. Lee, H.G. Kim, S.S. Kim, Enhancement of barrier properties of aluminum oxide layer by optimization of plasma-enhanced atomic layer deposition process, Thin Solid Films 534 (2013) 515.
[14] R.A. Wind, S.M. George, Quartz crystal microbalance studies of Al_2O_3 atomic layer deposition using trimethylaluminum and water at 125 °C, J. Phys. Chem. A 114 (2010) 1281.
[15] G. Dingemans, M.C.M. van de Sanden, W.M.M. Kessels, Influence of the deposition temperature on the c-Si surface passivation by Al_2O_3 films synthesized by ALD and PECVD, Electrochem. Solid-State Lett. 13 (3) (2010) H76.
[16] H. Kim, C. Cabral Jr., C. Lavoie, S.M. Rossnagel, Diffusion barrier properties of transition metal thin films grown by plasma-enhanced atomic-layer deposition, J. Vac. Sci. Technol. B 20 (4) (2002) 1321.
[17] A.S. da Silva Sobrinho, G. Czeremuszkin, M. Latrèche, M.R. Wertheimer, Defect-permeation correlation for ultrathin transparent barrier coatings on polymers, J. Vac. Sci. Technol. A 18 (1) (2000) 149.
[18] N. Kim, W.J. Postscavage Jr., A. Sundaramoothi, C. Henderson, B. Kippelen, S. Graham, A correlation study between barrier film performance and shelf lifetime of encapsulated organic solar cells, Sol. Energy Mater. Sol. Cells 101 (2012) 140.
[19] G. Rossi, M. Nulman, Effect of local flaws in polymeric permeation reducing barriers, J. Appl. Phys. 74 (1993) 5471.
[20] J.A. Bertrand, S.M. George, Evaluating Al_2O_3 gas diffusion barriers grown directly on Ca films using atomic layer deposition techniques, J. Vac. Sci. Technol. A 31 (2013) 01A122.
[21] H. Chatham, Oxygen diffusion barrier properties of transparent oxide coatings on polymeric substrates, Surf. Coat. Technol. 78 (1996) 1.
[22] A.A. Dameron, S.D. Davidson, B.B. Burton, P.F. Carcia, R.S. McLean, S.M. George, Gas diffusion barriers on polymers using multilayers fabricated by Al_2O_3 and rapid SiO_2 atomic layer deposition, J. Phys. Chem. C 112 (2008) 4573.
[23] C. Bishop, Roll-to-Roll Vacuum Deposition of Barrier Coating, John Wiley & Sons Inc, Hoboken, 2010. 73.